Multi-scale analysis of alkali–silica reaction (ASR): Impact of alkali leaching on scale effects affecting expansion tests

Stéphane Multon, Alain Sellier

Multi-scale analysis of Alkali-Silica Reaction (ASR): impact of alkali leaching on scale effects affecting expansion tests

Stéphane Multon [a*] and Alain Sellier [a]

(a) LMDC, Université de Toulouse, INSA, UPS, 135 Avenue de Rangueil, 31077 Toulouse cedex 04 France

Abstract

Alkali-silica reaction expansions are disturbed by a variety of mechanisms (alkali leaching, ASR-gel permeation through cracks, chemical conditions in pore solution water and its dependence on temperature, etc.). An important consequence is the difficulty of using the expansion test on specimens to analyse the behaviour of ASR-damaged structures. The paper focuses on the influence of leaching: alkali transport and consumption are modelled using a multi-scale approach (aggregate and concrete scales). The evaluation of the alkali concentration below which expansion stops is needed to perform relevant analysis in various alkali conditions and this alkali threshold is quantified according to calcium concentration and temperature. The impact of the coupling between alkali transport in aggregate and silica reactivity is also studied. Lastly, the consequences of leaching on ASR-expansion are analysed in two case studies drawn from the literature.

Keywords: alkali-silica reaction (ASR) (C), alkali (D), expansion (C), leaching, modelling (E)

[*] Corresponding author. *e-mail address:* multon@insa-toulouse.fr (Stéphane Multon)

1. Introduction

Expansion tests performed on mortar or concrete specimens are the most usual laboratory tool to evaluate the risk of Alkali-Silica Reaction in newly designed structures or to quantify the potential future expansion with a view to reassessing ASR-damaged structures. Several disturbing effects make the analysis of such tests difficult, by giving rise to scale effects. Alkali leaching [1]–[5], moisture gradient [6] and ASR-gel permeation through cracks [7]–[9] lead to larger expansions in larger specimens according to the storage conditions [5], [8]–[10]. These phenomena greatly impact the ASR-expansion measured on specimens, which raises the question of whether such measurements should be used to represent expansion in conditions existing in real structures. It is then necessary to analyse and quantify these effects so as to be able to use such usual tests as input data for structural assessment. It is difficult to estimate the contribution of each phenomenon to the differences of expansion with specimen size for the moment. In order to obtain a better prediction of expansion in structures, models have to be able to distinguish how much of the scale effect is due to alkali leaching and how much is induced by gel permeation through cracks for tests in leaching conditions. Expansion tests in the conditions the closest to structural reality are performed in a constant moist environment. For such experiments, one of the main scale effects is due to alkali leaching. This paper focuses on the alkali mass balance in ASR mechanisms and proposes modelling to reproduce the effect of alkali leaching on the expansion of prisms. The aim is to obtain a model that includes enough physical details to explain differences of expansion in conditions of alkali leaching but is simple enough to be usable for structural calculations.

Two equations are proposed to quantify alkali actions in ASR kinetics and expansion:

- At aggregate scale, the mass balance equation of alkalis takes their diffusion and fixation in ASR-gels in aggregates into account,
- At concrete scale, the mass balance considers the alkali diffusion in a specimen in relation to the boundary conditions, while the alkali consumption in the specimen is evaluated from the previous scale.

The link between chemical modelling and expansion is obtained through a model based on poromechanical theory that takes account of creep and damage at the concrete scale. The description of this mechanical part has been kept as brief as possible and only the main improvements compared to the previous version of this model are presented. In particular, the scaling up from gel pressure inside the aggregate to aggregate pressure on the surrounding concrete is modified. Finally, two case studies are presented to analyse literature experiments involving scale effects due to alkali leaching and potential consequences on measured expansion are discussed.

2. ASR mechanisms and alkali leaching

2.1 Multi-scale chemical approach

The chemical approach used in this paper is characterized by an alkali mass balance performed at two scales: the aggregate and the concrete scales (Figure 1).

At the aggregate scale, the alkali mass balance equation has to consider the diffusion and the fixation of alkali in ASR-gels. In order to be as representative as possible of the different types of aggregate attacks [11]–[13], analysis of ASR cannot consider the alkali diffusion in reactive aggregate as the only driving mechanism of ASR-kinetics. At least two main phenomena should be taken into consideration (Figure 1): ionic transport (to have alkali and silica in the same place) and the chemical reaction

(attack of silica to form gels). The impact of the coupling between alkali diffusion and silica reactivity on the distribution of ASR-gels in aggregate and concrete is analysed in the following part.

At concrete scale, the alkali diffusion equation takes the alkali flow $\overrightarrow{\varphi_{Na}^{c}}$ due to external boundary conditions into account (Figure 1). The alkali bound in ASR-gels ($S_{\sum Na_b}^{c}$ in Figure 1) can be evaluated as the sum of alkali flow at the boundary of the aggregate ($\overrightarrow{\varphi_{Na}^{agg}}\left(r = R_{agg}\right)$ in Figure 1) determined at the lower scale.

The alkali concentration in the cement paste at the aggregate edge and at the concrete scale ($[Na^{+}]_{x}$ in Figure 1) has to be the same in order for the multi-scale chemical approach to be consistent.

2.2 Alkali mass balance at aggregate scale

2.2.1 Alkali transport

The reactive silica is dissolved in presence of hydroxyl and alkali ions before ASR-gels are formed. In most cases, alkali and hydroxyl come from the cement paste solution and move to the silica in the aggregate to start the reaction. The mass balance equation at aggregate scales represents the alkali diffusion in aggregates and the alkali fixation in ASR-gels. It is applied for each size of aggregate, as proposed in previous modelling [14]–[17]. It can be written, for a constant water saturation degree:

$$p_{agg} S_r \frac{\partial [Na^{+}]}{\partial t} = -div\left(\overrightarrow{\varphi_{Na}^{agg}}\right) + S_{Na} \tag{1}$$

with p_{agg} the aggregate porosity, S_r the degree of water saturation, $[Na^{+}]$ the alkali concentration in solution, $\overrightarrow{\varphi_{Na}^{agg}}$ the alkali flow in the aggregate and S_{Na}, the rate of alkali binding in ASR-gels per unit of time and of aggregate volume.

The alkali flow depends on the coefficient of diffusion of alkali in the aggregate D_{agg}:

$$\overrightarrow{\varphi_{Na}^{agg}} = -D_{agg}\overrightarrow{grad}[Na^+] \quad (2)$$

For this diffusion phenomenon, the Arrhenius energy was taken to be 20 kJ/mol [18] to account for the increase of diffusion velocity with the temperature.

Despite the fact that alkali transport occurs in aggregate in diverse manners depending on whether the reactive silica is in contact with cracks or contained in veins of the aggregates [11], the coefficient of diffusion is assumed to be homogeneous in the aggregate. This is an approximation that requires a calibration by inverse analysis of expansion curves. The dependence of the expansion kinetics on the aggregate sizes can be reproduced by the differences of alkali ingress into the aggregate.

2.2.2 Alkali fixation in gels

Attack of silica and alkali fixation

The rate of alkali binding in ASR-gels (the sink term S_{Na} of the mass balance equation applied at the aggregate scale) is driven by the reactivity of the aggregate. In the absence of precise quantification of the different mechanisms involved in the aggregate attack, it is assumed that linear kinetics is sufficient to consider the silica attack and the ASR-gel precipitation according to an alkali threshold [17]. This is a simplified approach compatible with experimental results on pore solution extraction [19].

The form chosen for the rate of alkali fixation is similar to the one used in [17]:

$$S_{Na} = -\frac{\partial Na_f}{\partial t} = -\frac{\langle [Na^+] - [Na^+]_{(Ca,T)}^{thr} \rangle^+}{\tau_{ASR}} \quad (3)$$

with τ_{ASR} the characteristic time of silica attack, which can be considered to represent silica reactivity (even though, in reality, it combines both the kinetics of the reactive

silica dissolution and the kinetics of the ASR-gel production) and $[Na^+]^{thr}_{(Ca,T)}$ the alkali concentration "threshold" below which the reaction products cause negligible expansion. In the first version of this model [17], considering a constant threshold of alkali in equation (3) was necessary and sufficient to model the ASR-expansion of concrete with different alkali contents in moisture conditions [17]. But this same assumption leads to expansion rates that are too different for the expansion of specimens kept in NaOH solution and no threshold was taken into account for such calculations [9]. In fact, it is not really a threshold of silica attack, but an apparent threshold due to the difference of composition of the reaction products according to the calcium concentration [18]. The alkali concentration threshold, for which gel is no longer sufficiently expansive, is not constant as supposed in [17] but depends on the calcium concentration and the temperature, which can be approximated through the simplified approach proposed in the next part.

For this mechanism of reaction, the Arrhenius energy is taken to be 80 kJ/mol [20] to represent the dependence on thermal conditions.

Equation 3 leads to an evaluation of the alkali bound in ASR-gels. Usually, the molar ratio between silica (SiO2) and alkali (Na2O) present in gels in laboratory conditions is about 5 [21] [22]). The number of ASR-gel moles produced by the reaction is assumed to be equal to the number of moles of silica attacked by alkalis and can thus be deduced from the following equation:

$$\frac{\partial n_{gel}^{mol}}{\partial t} = \frac{5}{2}\frac{\partial Na_f}{\partial t} \tag{4}$$

Alkali threshold

Based on thermodynamics modelling, Kim and Olek showed that the formation of ASR-gels stopped when the alkali concentration became lower than a threshold value [18]. The rate of alkali binding (Equation 3) can be read as a simplified representation using only the alkali concentration to represent the disequilibrium:

- For high alkali concentration (high $[Na^+]$ / $[Ca^{2+}]$ ratio), the silica attack is rapid and large quantities of alkali are bound by gels. ASR-gel contains mainly alkali and silica [18] and is very expansive [23] [24].
- For lower alkali concentration, portlandite is dissolved and calcium concentration increases (decrease of $[Na^+]$ / $[Ca^{2+}]$ ratio). The rate of alkali binding decreases and gel becomes rich in calcium [18]. Such gels with high calcium content have low bound water contents [25] and could cause less expansion [23], [24].

In consequence, $[Na^+]^{thr}_{(Ca,T)}$, the alkali limit under which expansion stops, is not constant and has to be quantified according to the calcium concentration and the temperature. Based on the thermodynamic equilibrium of portlandite [16], calcium concentration (in mol/l) in the pore solution can be approximated from alkali concentration (in mol/l) and absolute temperature by [26]:

$$[Ca^{2+}] = 0.357 \cdot exp(386.8 \cdot [Na^+] - 0.01 \cdot T - 1.4 \cdot [Na^+] \cdot T) \quad (5)$$

The main interest of this simplified relation is that it enables calcium concentration to be evaluated from alkali and temperature. Thus, it is not necessary to model calcium diffusion, which limits the number of different variables in the numerical resolution.

Kim et al. [19] measured the evolution of alkali concentration in mortars subjected to ASR (Figure 2). From this experiment, it was possible to evaluate the alkali threshold at about 0.325 mol/l at 23°C. For such an alkali concentration and temperature,

Equation (5) gives a calcium concentration of about 0.11 mmol/l (Figure 3). At 23°C, if the alkali concentration becomes lower than 0.325 mol/l, Kim et al. show that expansion stops [19]. For this limit, the $[Na^+]$ / $[Ca^{2+}]$ ratio is around 3,000. Finally, $[Na^+]^{thr}_{(Ca,T)}$ can be defined as:

$$[Na^+]^{thr}_{(Ca,T)} = \rho^{(T)}_{sol} \cdot [Ca^{2+}] \quad (6)$$

$\rho^{(T)}_{sol}$, the $[Na^+]$ / $[Ca^{2+}]$ limit ratio, depends on the different solubility constants of the species acting in these processes (silica gels with more or less alkali and calcium) and thus on temperature since the variations of the constants with temperature are different [18].

If the $[Na^+]$ / $[Ca^{2+}]$ ratio is higher than $\rho^{(T)}_{sol}$, alkali ions are predominant and gels are very expansive (Figure 3). If calcium becomes preponderant compared to alkali (ratio lower than $\rho^{(T)}_{sol}$), expansive gel stops being produced [18]. Using Kim et al.'s experimental results ([19] – Figure 2), the ratio $\rho^{(T)}_{sol}$ can be evaluated for three temperatures (23, 38 and 55°C – Figure 2). It is interesting to note the good agreement of the variation of $\rho^{(T)}_{sol}$ determined from Kim et al.'s experiments with the Van't Hoff law for a standard enthalpy change of 205.9 kJ/mol (Figure 4), with $\rho^{(293)}_{sol}$ equal to 1.54e^3. This law was used to perform the following case studies.

With such equations, it is important to note that the alkali threshold is not constant even during a single expansion test at a uniform temperature. In the case of an expansion test without external supply of alkali:

- Alkali ions are first predominant and $[Na^+]^{thr}_{(Ca,T)}$ is equal to 0 at the beginning of the calculation,

- Then, alkalis are consumed in ASR-gels (and can be partly leached out) so alkali concentration in solution decreases, $[Na^+]^{thr}_{(Ca,T)}$ (Equation 6) increases with the calcium concentration (Equation 5). Finally, expansion stops when $[Na^+]^{thr}_{(Ca,T)}$ becomes higher than the alkali concentration in solution $[Na^+]$ (Equation 3).

In the case of expansion in NaOH solution, alkali concentration stays high and calcium concentration too low to stop the production of expansive gels. In such conditions, there is no apparent threshold as shown in [9]. This is well reproduced by the proposed relations since $[Na^+]^{thr}_{(Ca,T)}$ is then equal to 0 during the entire test ($[Ca^{2+}]$ close to 0 for high alkali concentration – Equation 5). It can be noted that this approach could also be useful for the quantification of the alkali effect in the control of ASR risk [27].

Finally, the different reactive processes involved in ASR are condensed into a single characteristic time to be calibrated on an expansion test.

2.2.3 Coupling transport / fixation in aggregates

In the proposed modelling, two main processes are assumed to drive the kinetics of alkali-silica reaction: transport in aggregate and reaction mechanisms (silica attack and gel formation). Each mechanism is represented by one parameter: the diffusion coefficient in aggregate for the transport, and the characteristic time of ASR for the reactions. Transport kinetics is also dependent on aggregate size: the larger the aggregate, the slower the penetration of ions into it (whatever the diffusion coefficient). Thus, the difference of kinetics of ASR-gel formation with aggregate size is smaller for a coefficient of diffusion of $1.^{e-13}$ m²/s (as measured in [28]) than for a

coefficient of $1.^{e-14}$ m²/s (Figure 5). The difference becomes all the greater as the aggregate size grows (Figure 5).

However, it is not possible to obtain a realistic expansion of concrete containing mixes of reactive aggregate with different sizes from this transport equation alone, as shown in [16]. With the assumption that transport in aggregate totally drives the ASR kinetics, calculations lead to an overestimate of the impact of the smallest reactive particles in alkali binding. This leads to an underestimate of the expansion of concrete containing both small and large aggregate [16]. Reaction kinetics is not directly dependent on aggregate size but depends on the alkali concentration in the aggregate (thus indirectly on transport). In consequence, if the transport is fast compared to the chemical reaction (Figure 6-a), the ASR-gel development is proportional to bound alkali and appears to be homogeneous in the aggregate (Figure 7-a). Expansion is then little impacted by aggregate size. This is the case for aggregate with low reactivity [29]. Conversely, more slowly diffusing aggregate with very reactive silica leads to a diffusion front in the aggregate until the threshold is reached (at about 500 days in Figure 6-b), and therefore to a steep gradient of bound alkali in the aggregate (Figure 7-b). Larger differences of expansion with aggregate size are observed [7] [30]. In reality, the front does not necessarily start from the external limit of the aggregate as in the simplified representation used in the model. It can also be a front starting from cracks existing in the aggregates before the ASR starts, as observed in [11]. Pore solution and alkali can move rapidly in such cracks, while the real diffusion impacting ASR-kinetics is a slower diffusion that takes place in the natural and less connected porosity of the aggregate.

In most cases, the role of the two mechanisms is important and has to be taken into account. The predominance of one equation over the other leads to behaviour that can

be more or less expansive for concrete containing a powder of small reactive particles, according to the aggregate nature [31]. To distinguish between the contribution of the diffusion and the contribution of the reaction kinetics, it is necessary to calibrate the expansion on tests with aggregates of different sizes.

2.3 Alkali mass balance at concrete scale

Experiments [1]–[5] have shown the importance of alkali leaching on ASR-expansion tests even in laboratory controlled conditions and at 95 % relative humidity. Consequently, ASR-expansion is not a uniform phenomenon even at the scale of the specimen (Figure 8). The analysis of such tests has to take the expansion gradient induced by the alkali gradient into account (Figure 1). The diffusion of alkali in concrete was determined by the usual mass balance:

$$p_c S_r \frac{\partial [Na^+]_c}{\partial t} = -div\left(\overrightarrow{\varphi_{Na}^c}\right) + S_{\sum Na_b}^c \tag{7}$$

with p_c the concrete porosity, S_r the degree of saturation (assumed constant), $[Na^+]_c$ the alkali concentration in the concrete solution, $\overrightarrow{\varphi_{Na}^c}$ the alkali flow at the specimen scale, and $S_{\sum Na_b}^c$ the sink term to account for alkali bound in ASR-gels at each time step determined at the aggregate scale.

The alkali flow in concrete depends on its coefficient of diffusion in the concrete:

$$\overrightarrow{\varphi_{Na}^c} = -D_c \ \overrightarrow{grad}[Na^+]_c \tag{8}$$

The Arrhenius energy was taken to be 40 kJ/mol [32] [33] to represent the influence of thermal conditions on diffusion with interaction with C-S-H in concrete.

The distribution of aggregate sizes is not homogeneous in specimens, and particularly, close to the concrete skin. This concrete heterogeneity can be the cause of expansion gradient between core and external surface. The impact of the aggregate sizes

distribution on ASR-expansion and cracking in specimens should be analysed through probabilistic approach in future work. By sake of simplicity, the assumption of homogeneous distribution is adopted in this work. The sink term of bound alkali can be calculated from the alkali flow in aggregate (Figure 1):

$$S^{c}_{\sum Na_b} = -\sum_{agg} N_{agg} \cdot 4\pi R^2_{agg} \cdot \varphi^{agg}_{Na}\left(r = R_{agg}\right) \tag{9}$$

with N_{agg} the number of reactive aggregates of each size per concrete volume, R_{agg} the aggregate size and $\varphi^{agg}_{Na}\left(r = R_{agg}\right)$ the alkali flow in the aggregate.

In the following calculations, the equations of transport in the aggregate and of ASR reaction (Equations (1) and (3), aggregate scale) and Equation (7) of global diffusion (concrete scale) are weakly coupled. The chemical approach proposed in the paper considers the diffusion in the specimen (top of Figure 8), takes the consumption of alkali ingress in aggregates into account (middle of Figure 8) and leads to the determination of the resulting gradient of volume of ASR-gels in the specimen (bottom of Figure 8). Due to the alkali gradient, the equations at the aggregate scale have to be solved at different points of the specimen. According to the kinetics of gel formation, the impact of alkali leaching can be more or less pronounced. The analysis is more difficult when the activation energies of the mechanisms involved are different. The acceleration of chemical reactions with temperature is larger than the acceleration of diffusive phenomena [18] [20]. In consequence, alkali leaching goes faster at high temperatures but the acceleration of chemical reactions is still greater and thus the consequences of alkali leaching cannot be directly compared without paying attention to the temperature conditions.

2.4 ASR pressure and concrete damage

The volume of ASR-gels was assessed by the multi-scale chemical approach. The consequences of the gel formation on concrete (expansion, damage) had to be analysed through mechanical considerations. From the volume of gels produced by the reaction, the mechanical effects on aggregate and concrete can be evaluated through various usual assumptions: imposed chemical strain [17] [34] [35] [36] or pressure [15], [37]–[43]. In this paper, the expansion is not obtained by the mechanical modelling proposed in [17] but through an existing poromechanical model previously developed and taking account of the damage and creep of concrete resulting from both external loading and internal pressure [44]. The consideration of creep during ASR-expansion is important to obtain a realistic evaluation of concrete damage [35] [44]. Concerning the mechanical aspect, the most important improvement compared to the previous modelling was the distinction between gel pressure in the aggregate and average aggregate pressure on the surrounding concrete (Figure 9). In most cases of ASR, cracking starts in the aggregate and aggregate cracks filled by the gel induce the cracking of the cement paste [11], [12] [45]. The consequences of ASR-gel formations were first assessed at the aggregate scale then deduced at the concrete scale (Figure 9).

2.4.1 Pressure in ASR-gels

At the aggregate scale (Figure 9), the gel pressure increases with the volumetric fraction of ASR-gels φ_{gel} (assumed to be proportional to the number of ASR-gel moles, determined by Equation (4) and to the molar volume of gels V_{gel}^{mol}) and decreases with the volumetric deformation of the aggregate due to elastic strain φ_{el}^{agg}

(elastic deformation of pore volume containing gels) and with the volumetric concrete cracking φ_{cr}^{c} (cracks are filled by ASR-gels).

It is also necessary to consider that a part of the volume of gel produced at the beginning of the reaction does not cause significant expansion. This can be established by two experimental observations:

- the absence of expansion for small reactive particles,
- the delay of expansion at the beginning of the reaction for large reactive particles, followed by a slope break of the expansion rate, whereas alkali consumption does not show any slope break but has an exponential evolution [19] as would be expected for equations of diffusion and reaction.

Several assumptions can explain this behaviour. Previous modelling assumed that it could be explained by the migration of ASR-gels in connected porosity very close to the reactive aggregate [14]–[17], [39], [41], [46]. This assumption appeared to be valid since very small distances were necessary to obtain good quantification (less than 10 µm) [17]. This assumption may be suitable for very reactive aggregate. In this case, the gels are first produced close to the cement paste and can partly migrate in the surrounding porosity [11], [47]–[49]. However, many reactive aggregates do not show any gels in cement paste before the first cracking [11], [12], [45], [49]. Other explanations concerning the aggregates characteristics effects can also be derived from fracture mechanics: cracks development in aggregate and resulting concrete cracking are dependant of the internal reactive silica distribution in aggregate, of the shape, of the size of aggregates relatively to the specimen ones, and of the distance of the aggregates from the edges. Moreover, very large aggregates expand due to the effect of a network of cracks developing in them; this aggregate cracking could make the expansion slower. These factors, not yet considered in the model, can explain a

part of the difference in the start of expansions curves between small and large aggregates. Chemical considerations could also explain the lack of expansion at the beginning of the reaction by the differences of expansive behaviour of ASR-products according to their time of formation. ASR-gels produced during the initial time of reaction could be less efficient to cause expansion [50]–[53]. This phenomenon can also be described as a non-expansive surface absorption of alkali by reactive silica at the beginning of the processes [54].

Consequently, a part of the gels produced by ASR, φ_{0_exp}, has to be removed from the total gel volume to represent this effect. Finally the pressure in ASR-gel can be written as:

$$p_{gel} = M_{gel} \cdot \left(\varphi_{gel} - \varphi_{0\_exp} - \varphi_{el}^{agg} - \varphi_{cr}^{c}\right) \tag{10}$$

with M_{gel} the Biot Modulus of gel in aggregate. As not all the porosity of aggregate is filled by ASR-gels, the Biot Modulus is assessed according to the volume of ASR-gels φ_{gel} contained by the aggregate as proposed by usual poromechanics [55]–[57].

The mechanisms resulting in only little expansion at the beginning of the reaction should be progressive. Therefore, the volume of ASR-gels leading to slight expansion at the beginning of the reaction was taken to be proportional to ASR-gel pressure as proposed in [58].

$$\varphi_{0\_exp} = \frac{4}{3}\pi\left(R_{agg}^{3} - \left(R_{agg} - t_{0\_exp}\right)^{3}\right) \cdot \frac{p_{gel}}{R_t} \tag{11}$$

with t_{0_exp} an average thickness to quantify the volume of the gels inefficient for expansion. This parameter was calibrated to obtain the volume of ASR-gels that had to be removed to obtain non-expansion of the smallest reactive particles and the delay in expansion for the largest.

With equation (11), gel pressure acts on the concrete as soon as gel is formed but the majority of the gel does not cause expansion until the gel pressure causes stress equal to the tensile strength of the material. Once the stress induced by this gel pressure exceeds the tensile strength, the volume of gels inefficient for expansion is assumed to be reached and all the supplementary gels cause pressure.

In poromechanics, the elastic volumetric deformation of pore volume containing gels φ_{el}^{agg} can be assessed by:

$$\varphi_{el}^{agg} = b_{gel} \cdot \varepsilon_{el}^{agg} \tag{12}$$

b_{gel} is the Biot coefficient due to gel formation in the aggregate. As for the Biot modulus, it is assessed according to the gel volume in the aggregate [55]–[57].

The volume of concrete cracks φ_{cr}^{c} can be assessed by plastic or damage modelling. The calibration of the parameters acting on the expansion level (V_{gel}^{mol} and t_{0_exp}) will be modified according to the capacity of the concrete to restrain the expansion due to gel formation [59]. Therefore, the parameters V_{gel}^{mol} and t_{0_exp} will depend on the assumptions of the mechanical modelling used and particularly on the assessment of the loss of rigidity due to cracking (with or without crack reclosure, consideration of creep, etc.). In the present work, the previous anisotropic damage modelling coupled with creep presented in [44] was used. However, the cracking criterion is on the gel pressure (equation 10) here, which causes aggregate cracking first and then leads to concrete cracking.

2.4.2 Resulting pressure in concrete

At the concrete scale (Figure 9), the volumetric deformation of aggregate under ASR-gel pressure, φ_{def}^{agg}, leads to the deformation of the concrete, which can be evaluated through the action of an equivalent pressure of aggregate on the concrete:

$$p_{agg} = M_{agg} \cdot \left(\varphi_{def}^{agg} - \varphi_{el}^{c}\right) \tag{13}$$

with M_{agg} the Biot Modulus of aggregate in concrete determined by usual poromechanics [55]–[57] and φ_{el}^{c} the elastic deformation of the concrete, and:

$$\varphi_{el}^{c} = b_{agg} \cdot \varepsilon_{el}^{c} \tag{14}$$

with b_{agg} the Biot coefficient of aggregate pressure on concrete (due to gel pressure in the aggregate). It is assessed according to the aggregate content in the concrete through usual poromechanics relationships [55]–[57]. It is thus possible to evaluate the gel pressure according to the conditions of compressibility of ASR-gels, aggregate and concrete.

Finally, the aggregate pressure on the concrete is linked to the gel pressure through:

$$p_{agg} = b_{gel} \cdot p_{gel} \tag{15}$$

As proposed in [43], [56], the poromechanical constitutive law then becomes:

$$\sigma = K_d^c \cdot (\varepsilon - \varepsilon_{an}) - \sum_{agg} b_{agg} \cdot p_{agg} \tag{16}$$

with K_d^c the concrete compressibility taking account of damage in the mechanical modelling used here, and ε_{an} the anelastic strains due to creep and cracking.

Finally, in the poromechanics approach proposed in this paper, the ASR-expansion of concrete results from two causes: the pressure due to the aggregate deformation under ASR-gel formation and the cracking induced by ASR-gels in the aggregate.

3. Case studies

The previous equations are now used to analyse two experiments in leaching conditions drawn from the literature. The first one is the well-documented experiment

on the impact of leaching on ASR-expansion performed by Lindgård [5], [60]. In this study, the alkali leaching and expansion were both evaluated on the same specimens. This provided data that was very interesting for the analysis of the effect according to specimen size and environmental storage. The second experiment is one used to evaluate the impact of the competition between diffusion into reactive aggregates and leaching out of the specimen. To simplify the analysis and the comparison, the values of the parameters depending on temperature are given for the reference temperature of 20°C. In the calculations, the values at storage temperature during the test are calculated through the Arrhenius law with the activation energies given in the first part of this paper.

3.1 Impact of leaching on expansion

The impact of leaching on ASR-expansion was analysed from experimental results obtained at 38°C on specimens with cross sections of 70x70 mm and 100x100 mm kept at 95% RH and in water [5], [60], [61]. The experiments gave alkali leaching (Figure 10) and measured expansion (Figure 11) over two years for the two sizes of specimens and for two moisture conditions (95% with limited leaching and in water with high leaching) [5]. The total alkali leaching (alkali content at the bottom of the storage containers and alkali content in the lining) was given at two time steps (1 and 2 years). For the other time steps, the alkali content at the bottom of the storage containers was given (but not the alkali content in the lining). To obtain data of the total leaching for intermediate time steps between the beginning and the first year and between the first and the second years, it was supposed that the ratio between alkali in the containers and total leached alkali was the same throughout the experiments (Figure 10).

The first difficulty encountered in analysing the results was to represent the external conditions of leaching. The storage at 95% RH does not give a boundary condition that is easy to model for alkali external diffusion since such storage should not lead to leaching. In reality, the leaching was due to the condensation of water vapour on the surfaces of specimens following small temperature variations during the tests. The boundary condition was obtained by inverse analysis of the total leached alkali given by experiments (Figure 10). As alkali bound by ASR-gels influences this total amount of leached alkali, the inverse analysis of boundary conditions and the calibration of expansion parameters were performed simultaneously for the most limited leaching (specimens with cross section of 100x100 mm kept at 95% RH). Once expansion parameters had been determined for these conditions (Table 1), only the boundary conditions were modified to obtain the other leaching curves (Figure 10 – storage in water and specimens with cross sections of 70x70 mm) with no modification of the expansion parameters. With good reproduction of leaching results (Figure 10), ASR-expansions calculated by the previous equations were in good agreement with expansions measured during experiments (Figure 11). The differences of expansion for the two sizes of specimens studied in [5] could be quantified by the differences of ASR-advancement in specimens (Figure 12) due to alkali leaching. In the specimens with severe conditions of leaching, expansion stopped when the alkali concentration dropped below the alkali threshold obtained through Equations (5) and (6) (for 38°C, the alkali threshold is estimated at about 260 mmol/l). This analysis validated the simplified representation of the alkali threshold for the assessment of ASR-expansion in various alkali conditions. Moreover, the decrease of expansion with the specimen size could then be explained by the alkali leaching alone. In this case, it was not useful to assess the volume of gels lost by permeation through cracks as for

experiments on specimens kept in alkali solution [9]. This effect of gel permeation appeared to be negligible compared with the alkali leaching effect for the sizes of specimens and the conditions of this experiment. Lastly, modelling can assess a theoretical value of expansion which could appear in concrete if no leaching occurred (Figure 11) within the outlines of the assumptions proposed here. This is an important value for structural analysis since, in the core of large damaged structures, leaching should be negligible. However, it cannot be stated that it will represent the real expansion in damaged structures, because of environmental conditions (moisture conditions, temperature effects on viscosity and/or molar volume of ASR-gels, mechanical conditions) or other disturbing effects (gel permeation through cracks). The modelling confirms the large impact of alkali leaching on ASR-expansion measured on specimens. Commonly used expansion tests should not be extrapolated to large structures without using multi-scale analysis.

3.2 Competition between alkali diffusion in aggregate and external leaching

The previous equations were finally used to analyse the pessimum effect of expansion with aggregate size [62]–[64]. The pessimum effect obtained in [59] can be reproduced by the previous equations (Figure 13 and Figure 14) with a single set of parameters (Table 1) and thus could be explained by alkali leaching in conditions of moisture similar to Lindgård's ones (95% RH). Obtaining smaller expansion for larger reactive aggregate can then be explained by the competition between alkali diffusion in the aggregate and external leaching. The time necessary for alkali to reach the core of the aggregate is longest for the largest aggregates. At the same time, part of the alkali is leached out of the specimens. The result of the competition between

the two transport systems is that a larger amount of alkali is leached for concrete containing larger reactive aggregate and thus smaller resulting expansion even after a long time of stabilization of the phenomena (Figure 13).

Differences can be noted between the parameters of the first case study and this one (Table 1). For the diffusion in the aggregate, characteristic time of silica attack and thickness of non-expansive gels, they could be explained by differences in the nature and size of the reactive aggregates. The difference of molar volume of ASR-gels can be due to the effect of storage temperature on the composition of gels (differences of expansion with temperature were observed on the concrete studied in Lindgård's experiments [5]). This second study confirms, by calculations, that the pessimum effect with aggregate size in leaching conditions could be due to the competition between diffusion into the aggregate and alkali diffusion out of the specimens. However this remains theoretical since no leaching data was available and a pessimum effect can exist even when leaching is impossible (storage in alkali solutions [9]). Experiments with different sizes of reactive aggregate and control of alkali leaching would be necessary to estimate the proportions of expansion decrease that are due to alkali leaching and to gel permeation (which is the explanation proposed in the case of storage in alkali solution) and finally to validate such modelling.

4. Conclusion

Alkali-silica reaction expansion tests can be disturbed by several phenomena in laboratory conditions. One of the main consequences is the difficulty of using expansion tests on specimens to analyse the behaviour of ASR-damaged structures.

Modelling has to take these effects into account to help in the analysis of laboratory tests and to make the link between experimentation on specimens and structural diagnosis. Scale-up methods have been used and combined to quantify the phenomenon (alkali diffusion and chemical reactions at the aggregate scale, alkali transport at the specimen scale taking into account the alkali consumption from the lower scale). At the aggregate scale, a mass balance equation with a sink term is necessary to obtain simplified but realistic kinetics of ASR-expansion. The alkali transport in aggregate is necessary to reproduce the dependence of the ASR kinetics on size for aggregates with high and intermediate reactivity. The sink term depending on alkali concentration is necessary to represent alkali fixation and to reproduce ASR kinetics of aggregates with low reactivity and mixes of reactive aggregate of different sizes (particularly the impact of the finest reactive particles for aggregates with intermediate reactivity).

The main interest of the present work lies in:

- The possibility to assess the apparent alkali threshold according to temperature and calcium concentration with simplified equations. Thus the alkali threshold defined in the first modelling [17] can be explained by the conditions of equilibrium between alkali and calcium ions [18]. Alkali concentration below which there is no expansion is not a threshold in silica attack but a concentration under which gels contain mainly calcium and are not significantly expansive. Differences of expansions on specimens in leaching conditions drawn from literature have been reproduced using the proposed equations to assess the alkali threshold.
- The analysis of the impact of the coupling between alkali transport in aggregate (characterized by a coefficient of diffusion) and silica reactivity

(determined through a characteristic time of silica attack) on ASR-gel production to reproduce kinetics according to aggregate size and distribution. The volume of gels thus calculated can be used in mechanical modelling.

- The combination of the mass balance at aggregate scale with the alkali transport at the concrete scale taking the alkali diffusion in aggregate, the binding of alkali in ASR-gels and the alkali diffusion out of specimens into account simultaneously. Due to the high mobility of alkali ions, alkali leaching should not be neglected in ASR-modelling, particularly when analysing expansions in specimens, since it induces a significant expansion gradient between the core and the external surface.

After the development of modelling at the aggregate scale [15]–[17], this work is a second step to obtain the capacity to analyse ASR-expansion in specimens kept in usual conditions in the laboratory. Based on this multi-scale modelling, it is possible to analyse the causes of the ASR scale effect due to alkali leaching, which can induce differences of expansion with specimen sizes. The next step will be to consider the permeation of ASR-gels through cracks.

Acknowledgement

The authors would like to thank Jan Lindgård for verifying the data used in part 3.1 'Impact of leaching on expansion'.

References

[1] C. A. Rogers and R. D. Hooton, "Reduction in mortar and concrete expansion with reactive aggregates due to alkali leaching," *Cem Concr Agg*, vol. 13, no. 1, pp. 42–49, 1991.

[2] J. Duchesne and M. A. Bérubé, “Long-term effectiveness of supplementary cementing materials against alkali-silica reaction,” *Cem. Concr. Res.*, vol. 31, pp. 1057–1063, 2001.

[3] P. Rivard, M. A. Bérubé, J. P. Ollivier, and G. Ballivy, “Alkali mass balance during the accelerated concrete prism test for alkali-aggregate reactivity,” *Cem. Concr. Res.*, vol. 33, pp. 1147–1153, 2003.

[4] P. Rivard, M. A. Bérubé, J.-P. Ollivier, and G. Ballivy, “Decrease of pore solution alkalinity in concrete tested for alkali-silica reaction,” *Materials and Structures*, vol. 40. pp. 909–921, 2007.

[5] J. Lindgård, E. J. Sellevold, M. D. A. Thomas, B. Pedersen, H. Justnes, and T. F. Rønning, “Alkali-silica reaction (ASR) - Performance testing: Influence of specimen pre-treatment, exposure conditions and prism size on alkali leaching and prism expansion,” *Cem. Concr. Res.*, vol. 53, pp. 68–90, 2013.

[6] S. Poyet, A. Sellier, B. Capra, G. Thèvenin-Foray, J. M. Torrenti, H. Tournier-Cognon, and E. Bourdarot, “Influence of Water on Alkali-Silica Reaction: Experimental Study and Numerical Simulations,” *J. Mater. Civ. Eng.*, vol. 18, no. August, pp. 588–596, 2006.

[7] D. W. Hobbs and W. H. Gutteridge, “Particle size of aggregate and its influence upon the expansion caused by the alkali–silica reaction,” *Mag. Concr. Res.*, vol. 31, no. 109, pp. 235–242, 1979.

[8] N. Z. C. Zhang, A. Wang, M. Tang, “Influence of dimension of test specimen on alkali aggregate reactive expansion,” *ACI Mater. J.*, vol. 96, pp. 204–207, 1999.

[9] X. X. Gao, S. Multon, M. Cyr, and A. Sellier, “Alkali-silica reaction (ASR) expansion: Pessimum effect versus scale effect,” *Cem. Concr. Res.*, vol. 44, pp. 25–33, 2013.

[10] Bakker RFM, “The influence of test specimen dimensions on the expansion of reactive alkali aggregate in concrete,” in *Proceedings of the 6th ICAAR, Copenhagen, Denmark*, 1983, pp. 369–375.

[11] J. M. Ponce and O. R. Batic, “Different manifestations of the alkali-silica reaction in concrete according to the reaction kinetics of the reactive aggregate,” *Cem. Concr. Res.*, vol. 36, pp. 1148–1156, 2006.

[12] M. Ben Haha, E. Gallucci, A. Guidoum, and K. L. Scrivener, “Relation of expansion due to alkali silica reaction to the degree of reaction measured by SEM image analysis,” *Cem. Concr. Res.*, vol. 37, pp. 1206–1214, 2007.

[13] J. Berard, R. Roux, I. Depuis, and C. Climinces, “La viabilite des betons du Quebec: le role des granulats,” *Can J Civ Eng*, vol. 13, no. 1, pp. 12–24, 1986.

[14] Y. Furusawa, H. Ohga, and T. Uomoto, “An analytical study concerning prediction of concrete expansion due to alkali–silica reaction,” in*: Malhotra (Ed.), 3rd Int. Conf. on Durability of Concrete, Nice, France*, 1994, pp. 757–780, SP 145–40.

[15] A. Suwito, W. Jin, Y. Xi, and C. Meyer, “A Mathematical Model for the Pessimum Size Effect of ASR in Concrete,” *Civ. Eng.*, pp. 1–29.

[16] S. Poyet, A. Sellier, B. Capra, G. Foray, J.-M. Torrenti, H. Cognon, and E. Bourdarot, “Chemical modelling of Alkali Silica reaction: Influence of the reactive aggregate size distribution,” *Mater. Struct.*, vol. 40, pp. 229–239, 2007.

[17] S. Multon, A. Sellier, and M. Cyr, “Chemo-mechanical modeling for prediction of alkali silica reaction (ASR) expansion,” *Cem. Concr. Res.*, vol. 39, pp. 490–500, 2009.

[18] T. Kim and J. Olek, “Chemical sequence and kinetics of alkali-silica reaction part II. A thermodynamic model,” *J. Am. Ceram. Soc.*, vol. 97, pp. 2204–2212, 2014.

[19] T. Kim, J. Olek, and H. Jeong, “Alkali–silica reaction: Kinetics of chemistry of pore solution and calcium hydroxide content in cementitious system,” *Cem. Concr. Res.*, vol. 71, pp. 36–45, 2015.

[20] D. Bulteel, E. Garcia-Diaz, C. Vernet, and H. Zanni, “Alkali–silica reaction: A Method to quantify the reaction degree,” *Cem. Concr. Res.*, vol. 32, pp. 1199–1206, 2002.

[21] M. Kawamura and H. Fuwa, “Effects of lithium salts on ASR gel composition and expansion of mortars,” *Cem. Concr. Res.*, vol. 33, no. February 2001, pp. 913–919, 2003.

[22] A. Leemann and P. Lura, “E-modulus of the alkali-silica-reaction product determined by micro-indentation,” *Constr. Build. Mater.*, vol. 44, pp. 221–227, 2013.

[23] T. C. Powers and H. H. Steinour, “An interpretation of some published researches on the Alkali-Aggregate Reaction - Part 1: The chemical reactions and mechanism of expansion,” *J. Am. Concr. Inst.*, vol. 26, no. 6, pp. 497–516, 1955.

[24] M. Prezzi, P. J. M. Monteiro, and G. Sposito, “The alkali-silica reaction, part I: Use of the double-layer theory to explain the behavior of reaction-product gels,” *ACI Mater. J.*, vol. 94, no. 94, pp. 10–17, 1997.

[25] A. Leemann, G. Le Saout, F. Winnefeld, D. Rentsch, and B. Lothenbach, “Alkali-Silica reaction: The Influence of calcium on silica dissolution and the formation of reaction products,” *J. Am. Ceram. Soc.*, vol. 94, pp. 1243–1249, 2011.

[26] M. Salgues, A. Sellier, S. Multon, E. Bourdarot, and E. Grimal, “DEF modelling based on thermodynamic equilibria and ionic transfers for structural analysis,” *Eur. J. Environ. Civ. Eng.*, vol. 18, no. 4, pp. 1–26, 2014.

[27] I. Moundoungou, D. Bulteel, E. Garcia-Diaz, V. Thiéry, P. Dégrugilliers, and J. G. Hammerschlag, “Reduction of ASR expansion in concretes based on reactive chert aggregates: Effect of alkali neutralisation capacity,” *Constr. Build. Mater.*, vol. 54, pp. 147–162, 2014.

[28] S. Goto and D. M. Roy, “Diffusion of ions through hardened cement pastes,” *Cem. Concr. Res.*, vol. 11, pp. 751–757, 1981.

[29] C. F. Dunant and K. L. Scrivener, “Effects of aggregate size on alkali-silica-reaction induced expansion,” *Cem. Concr. Res.*, vol. 42, pp. 745–751, 2012.

[30] L. F. M. Sanchez, S. Multon, A. Sellier, M. Cyr, B. Fournier, and M. Jolin, “Comparative study of a chemo–mechanical modeling for alkali silica reaction (ASR) with experimental evidences,” *Constr. Build. Mater.*, vol. 72, pp. 301–315, 2014.

[31] A. Carles-Gibergues, M. Cyr, M. Moisson, and E. Ringot, “A simple way to mitigate alkali-silica reaction,” *Mater. Struct.*, vol. 41, pp. 73–83, 2007.

[32] H. Liang, L. Li, N. D. Poor, and a. a. Sagüés, “Nitrite diffusivity in calcium nitrite-admixed hardened concrete,” *Cem. Concr. Res.*, vol. 33, pp. 139–146, 2003.

[33] T. de Larrard, F. Benboudjema, J. B. Colliat, J. M. Torrenti, and F. Deleruyelle, "Concrete calcium leaching at variable temperature: Experimental data and numerical model inverse identification," *Comput. Mater. Sci.*, vol. 49, no. 1, pp. 35–45, 2010.

[34] C. F. Dunant and K. L. Scrivener, "Micro-mechanical modelling of alkali-silica-reaction-induced degradation using the AMIE framework," *Cem. Concr. Res.*, vol. 40, no. 4, pp. 517–525, 2010.

[35] A. B. Giorla, K. L. Scrivener, and C. F. Dunant, "Influence of visco-elasticity on the stress development induced by alkali–silica reaction," *Cem. Concr. Res.*, vol. 70, pp. 1–8, 2015.

[36] M. Alnaggar, G. Cusatis, and G. Di Luzio, "Lattice Discrete Particle Modeling (LDPM) of Alkali Silica Reaction (ASR) deterioration of concrete structures," *Cem. Concr. Compos.*, vol. 41, pp. 45–59, 2013.

[37] P. Goltermann, "Mechanical Predictions on Concrete Deterioration . Part 1 : Eigenstresses in Concrete," *ACI Mater. J.*, no. 91, pp. 543–550, 1995.

[38] A. Nielsen, F. Gottfredsen, and F. Thøgersen, "Development of stresses in concrete structures with alkali-silica reactions," *Mater. Struct.*, vol. 26, pp. 152–158, 1993.

[39] Z. P. Bazant and A. Steffens, "Mathematical model for kinetics of alkali-silica reaction in concrete," *Cem. Concr. Res.*, vol. 30, pp. 419–428, 2000.

[40] W. Puatatsananon and V. Saouma, "Chemo-mechanical micromodel for alkali-silica reaction," *ACI Mater. J.*, vol. 110, no. 110, pp. 67–77, 2013.

[41] L. Charpin and A. Ehrlacher, "A computational linear elastic fracture mechanics-based model for alkali-silica reaction," *Cem. Concr. Res.*, vol. 42, no. 4, pp. 613–625, 2012.

[42] R. Pignatelli, C. Comi, and P. J. M. Monteiro, "A coupled mechanical and chemical damage model for concrete affected by alkali-silica reaction," *Cem. Concr. Res.*, vol. 53, pp. 196–210, 2013.

[43] L. Charpin and A. Ehrlacher, "Microporomechanics study of anisotropy of ASR under loading," *Cem. Concr. Res.*, vol. 63, pp. 143–157, 2014.

[44] E. Grimal, A. Sellier, S. Multon, Y. Le Pape, and E. Bourdarot, "Concrete modelling for expertise of structures affected by alkali aggregate reaction," *Cem. Concr. Res.*, vol. 40, no. 4, pp. 502–507, 2010.

[45] L. F. M. Sanchez, B. Fournier, M. Jolin, and J. Duchesne, "Reliable quantification of AAR damage through assessment of the Damage Rating Index (DRI)," *Cem. Concr. Res.*, vol. 67, pp. 74–92, 2015.

[46] A. Sellier, J. P. Bournazel, and A. Mébarki, "Une modélisation de la réaction alcalis-granulat intégrant une description des phénomènes aléatoires locaux," *Mater. Struct.*, vol. 28, no. 1, pp. 373–383, 1995.

[47] R. Pouhet and M. Cyr, "Alkali–silica reaction in metakaolin-based geopolymer mortar," *Mater. Struct.*, vol. 48, pp. 571–583, 2014.

[48] R. Idir, M. Cyr, and A. Tagnit-Hamou, "Use of fine glass as ASR inhibitor in glass aggregate mortars," *Constr. Build. Mater.*, vol. 24, no. 7, pp. 1309–1312, 2010.

[49] G. Giaccio, R. Zerbino, J. M. Ponce, and O. R. Batic, “Mechanical behavior of concretes damaged by alkali-silica reaction,” *Cem. Concr. Res.*, vol. 38, pp. 993–1004, 2008.

[50] T. Ichikawa and M. Miura, “Modified model of alkali-silica reaction,” *Cem. Concr. Res.*, vol. 37, pp. 1291–1297, 2007.

[51] T. Ichikawa, “Alkali-silica reaction, pessimum effects and pozzolanic effect,” *Cem. Concr. Res.*, vol. 39, pp. 716–726, 2009.

[52] V. E. Saouma, R. A. Martin, M. A. Hariri-Ardebili, and T. Katayama, “A mathematical model for the kinetics of the alkali–silica chemical reaction,” *Cem. Concr. Res.*, vol. 68, pp. 184–195, 2015.

[53] E. Garcia-Diaz, J. Riche, D. Bulteel, and C. Vernet, “Mechanism of damage for the alkali-silica reaction,” *Cem. Concr. Res.*, vol. 36, pp. 395–400, 2006.

[54] E. Garcia-Diaz, D. Bulteel, Y. Monnin, P. Degrugilliers, and P. Fasseu, “ASR pessimum behaviour of siliceous limestone aggregates,” *Cem. Concr. Res.*, vol. 40, no. 4, pp. 546–549, 2010.

[55] O. Coussy, *Poromechanics*, Wiley. New York, 2004.

[56] L. Dormieux, D. Kondo, and F. Ulm, *Microporomechanics*, Wiley. 2006.

[57] O. Coussy and P. J. M. Monteiro, “Poroelastic model for concrete exposed to freezing temperatures,” *Cem. Concr. Res.*, vol. 38, pp. 40–48, 2008.

[58] A. Sellier, J. P. Bournazel, and A. Mébarki, “Une modélisation de la réaction alcalis-granulat intégrant une description des phénomènes aléatoires locaux,” *Mater. Struct.*, vol. 28, no. 7, pp. 373–383, 1995.

[59] S. Multon, M. Cyr, A. Sellier, P. Diederich, and L. Petit, “Effects of aggregate size and alkali content on ASR expansion,” *Cem. Concr. Res.*, vol. 40, pp. 508–516, 2010.

[60] J. Lindgård, “Alkali–silica reactions (ASR)—Performance testing,” NTNU, Norwegian University of Science and Technology, Trondheim, Norway, 2013.

[61] J. Lindgård, E. J. Sellevold, M. D. A. Thomas, B. Pedersen, H. Justnes, and T. F. Rønning, “Alkali-silica reaction (ASR) - Performance testing: Influence of specimen pre-treatment, exposure conditions and prism size on concrete porosity, moisture state and transport properties,” *Cem. Concr. Res.*, vol. 53, pp. 145–167, 2013.

[62] Z. Xie, W. Xiang, and Y. Xi, “ASR Potentials of Glass Aggregates in Water-Glass Activated Fly Ash and Portland Cement Mortars,” *J. Mater. Civ. Eng.*, vol. 15, no. 1, pp. 67–74, 2003.

[63] X. Zhang and G. W. Groves, “The alkali-silica reaction in OPC/silica glass mortar with particular reference to pessimum effects,” *Adv. Cem. Res.*, vol. 3, no. 9, pp. 9–13, 1990.

[64] K. Ramyar, A. Topal, and O.¨Andiç, “Effects of aggregate size and angularity on alkali-silica reaction,” *Cem. Concr. Res.*, vol. 35, pp. 2165–2169, 2005.

Table

Table **1**: Parameters for the calculations presented in the two case studies for the reference temperature of 20°C

		Lindgård et al.	Multon et al.
T	storage temperature (°C)	38°C	60°C
D_c	alkali diffusion in concrete (m²/s)	1.e-12	1.e-12
D_{agg}	transport in aggregate (m²/s)	1.35e-15	0.4e-15
τ_{ASR}	characteristic time of silica attack (day)	400.	1200.
t_{0_exp}	thickness of non-expansive gels (µm)	12.	5.
V_{gel}^{mol}	molar volume of ASR-gels (cm^3/mol)	105.	71.

Figures

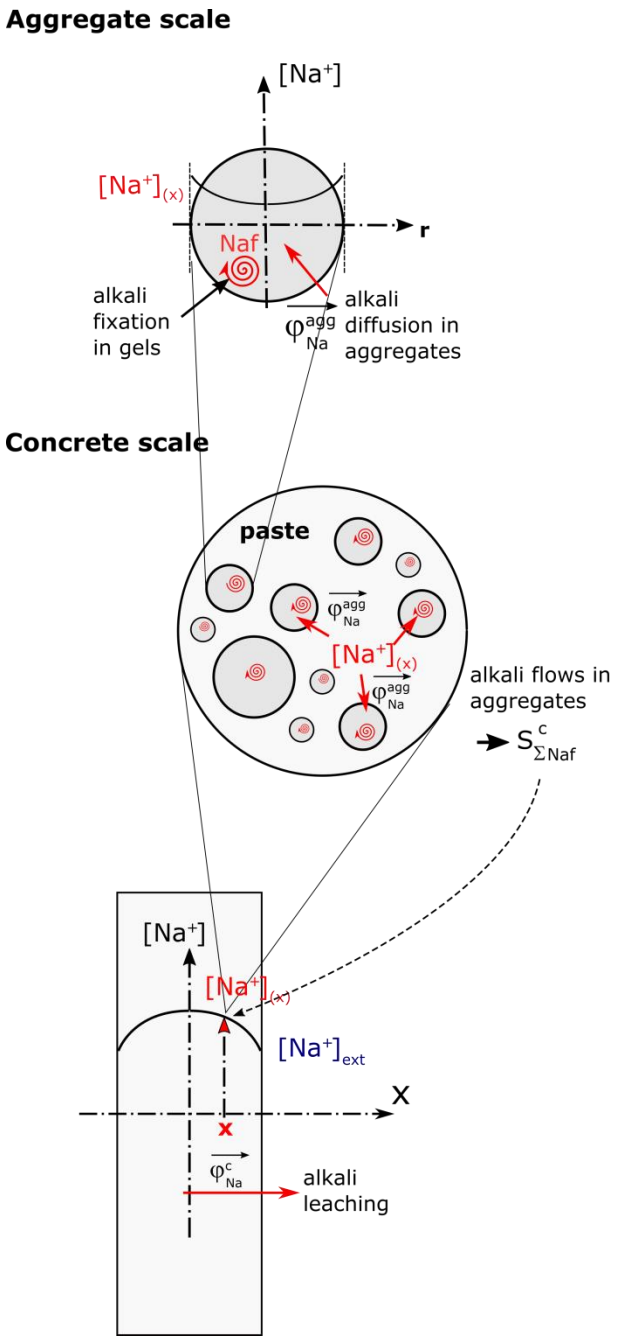

Figure 1: Alkali mass balance at aggregate scale (with diffusion and fixation in ASR-gels), at concrete scale and at specimen scale (diffusion in the specimen)

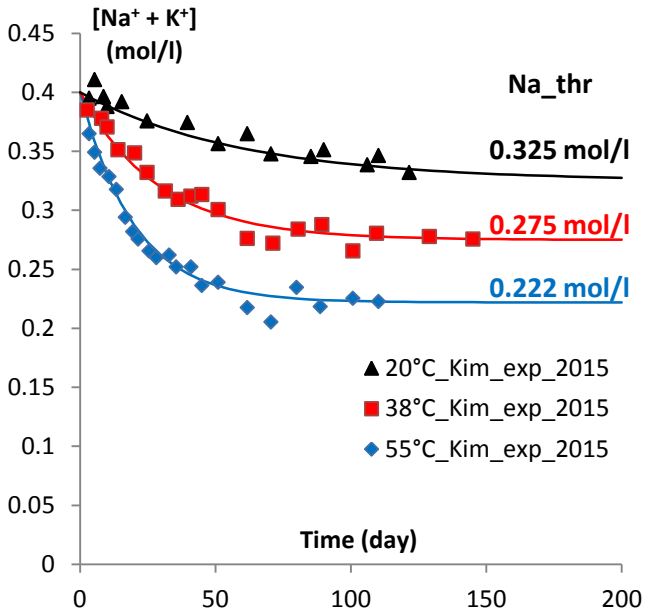

Figure 2: Evolution of alkali concentration in mortars subjected to ASR for three temperatures (experimental results from Kim et al., 2015 [19])

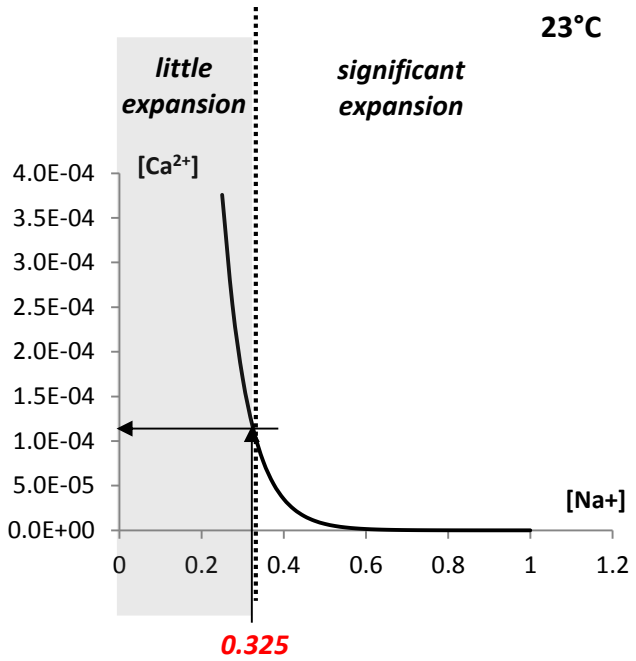

Figure 3: Calcium concentration (mol/l) according to alkali concentration (mol/l) in solution at 23°C due to portlandite equilibrium and limit of expansion of ASR-gels

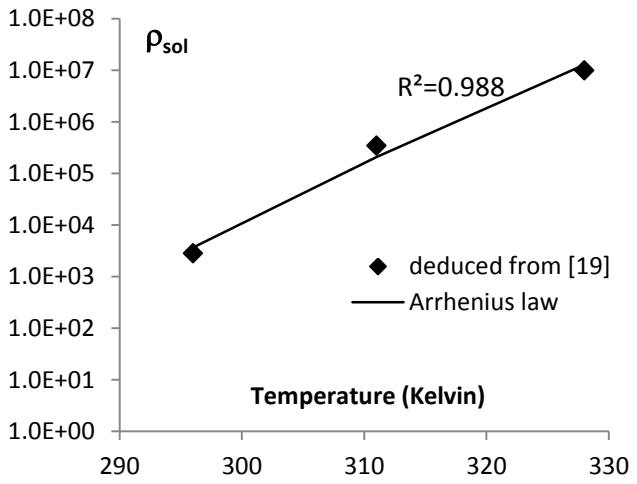

Figure 4: Evolution of $\boldsymbol{\rho_{sol}^{(T)}}$ for the determination of alkali threshold with temperature

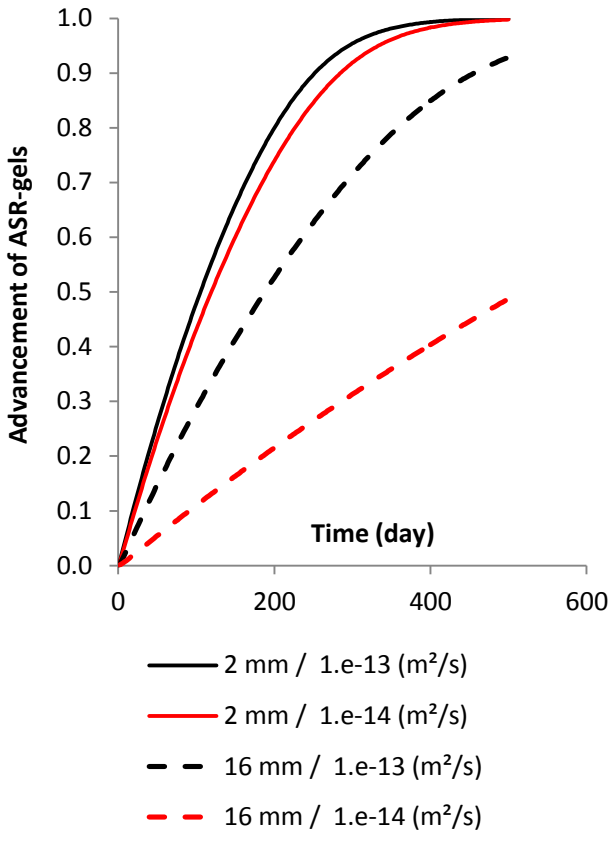

Figure 5: Kinetics of gel formation for coefficients of diffusion of $1.^{e-13}$ m²/s and $1.^{e-14}$ m²/s and the same characteristic time of reaction of 500 days for two sizes of aggregate (mean diameters 2 and 16 mm)

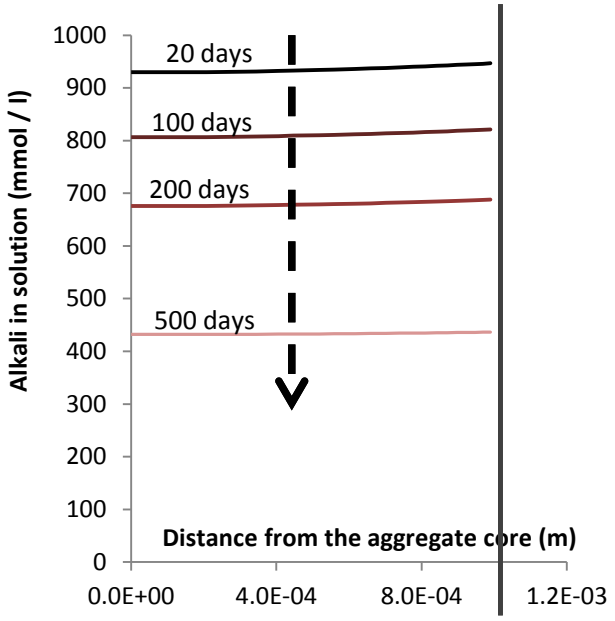

(a)

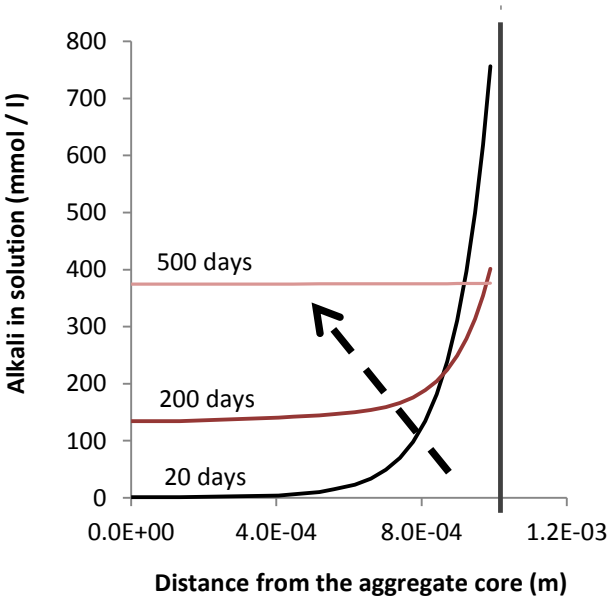

(b)

Figure **6**: Profiles of free alkali in an aggregate of mean diameter of 2 mm: (a) coefficient of diffusion of $1.^{e-13}$ m²/s and characteristic time of reaction of 1000 days, (b) coefficient of diffusion of $1.^{e-15}$ m²/s and characteristic time of reaction of 100 days

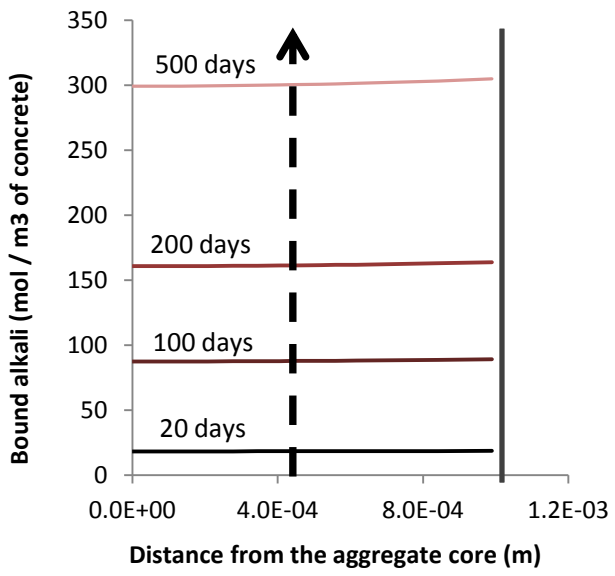

(a)

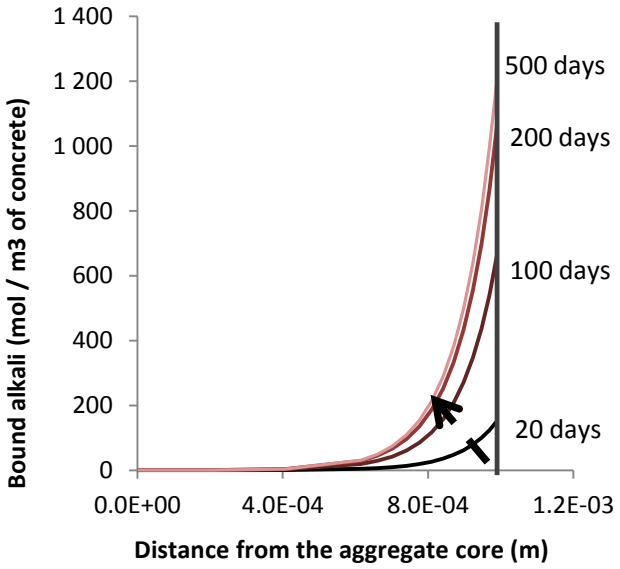

(b)

Figure 7: Profiles of alkali bound in ASR-gels for an aggregate of mean diameter of 2 mm: (a) coefficient of diffusion of $1.^{e-13}$ m²/s and characteristic time of reaction of 1000 days, (b) coefficient of diffusion of $1.^{e-15}$ m²/s and characteristic time of reaction of 100 days

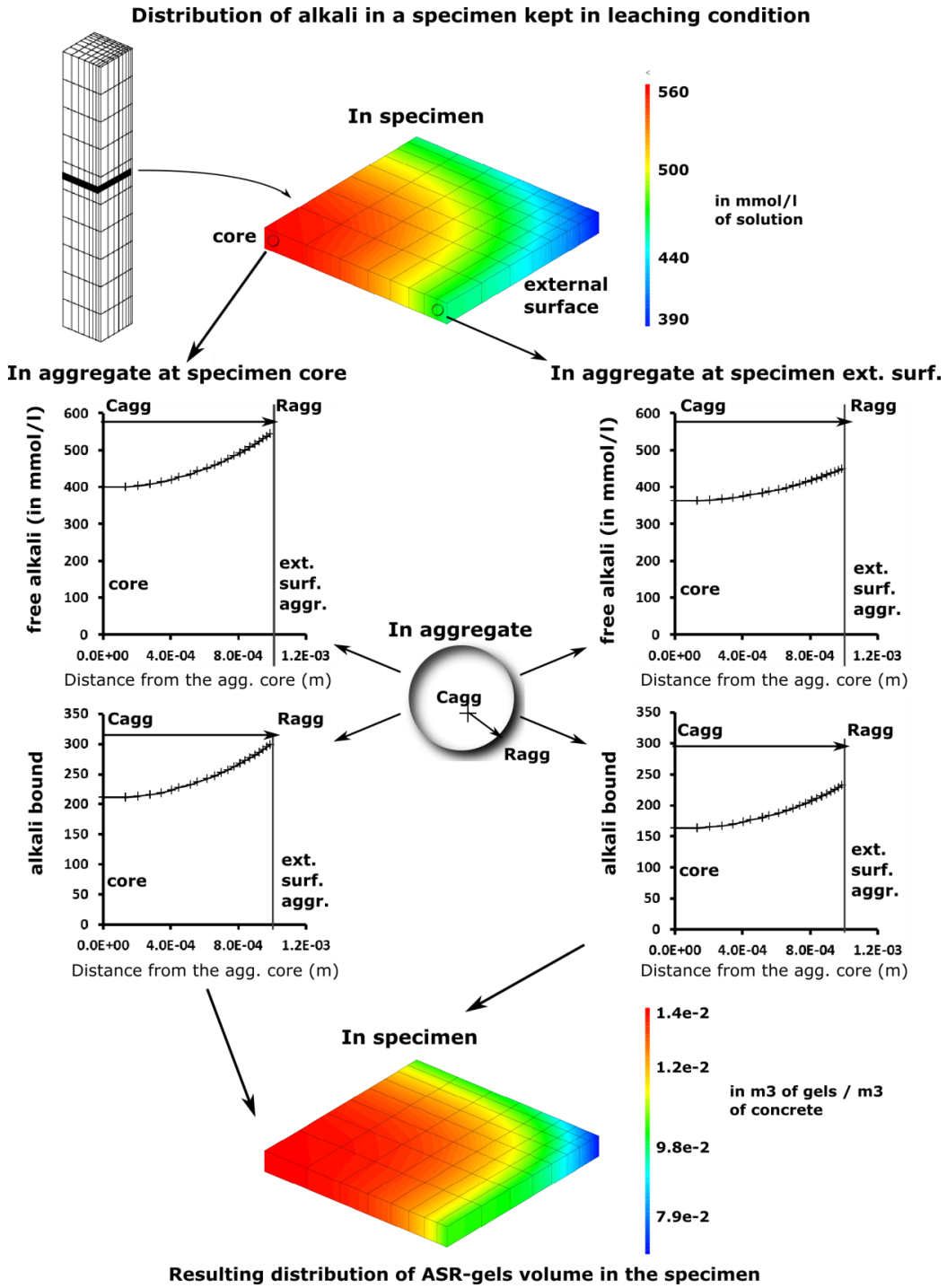

Figure 8: Slices of specimens (100x100 mm cross section) subjected to ASR in moderate leaching condition (aggregate coefficient of diffusion of $1.^{e-14}$ m²/s and characteristic time of reaction of 500 days). Top: distribution of alkali in specimen, middle: gradient of free and bound alkali in aggregates in the core and at the external surface of the specimen, bottom: resulting distribution of ASR-gels in specimen

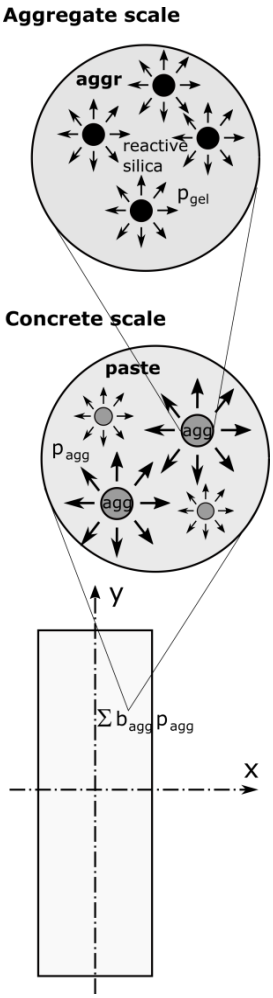

Figure **9**: Pressure induced by ASR-gels in aggregate and resulting pressure in concrete

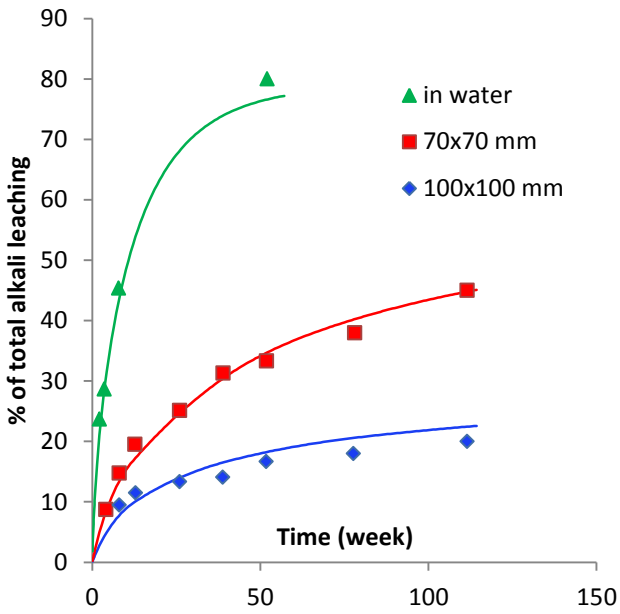

Figure **10**: Total alkali leaching according to specimen size and storage in Lindgard's experiments [5] (points) and numerical modelling (curves)

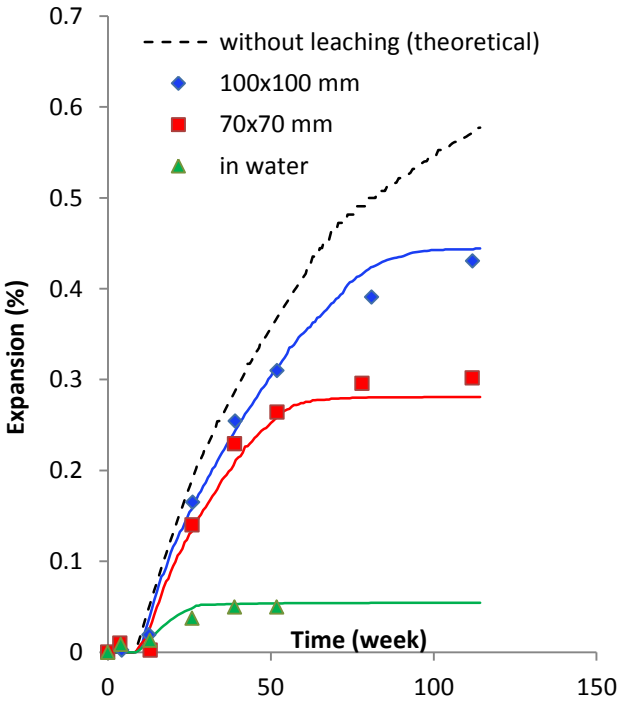

Figure **11**: Expansion according to specimen size and storage in Lindgard's experiments [5] (points) and numerical modelling (curves)

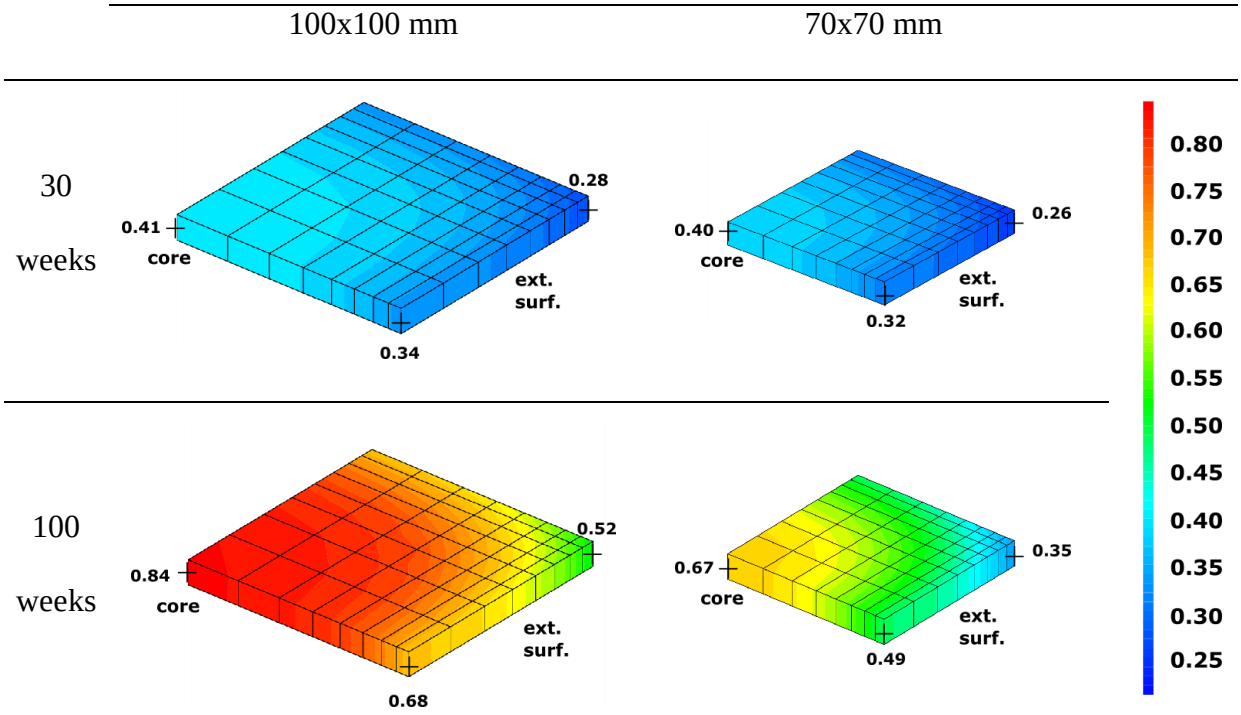

Figure **12**: Advancement of ASR in one size of aggregate in the specimens of Lindgard's experiments [5] after 30 and 100 weeks

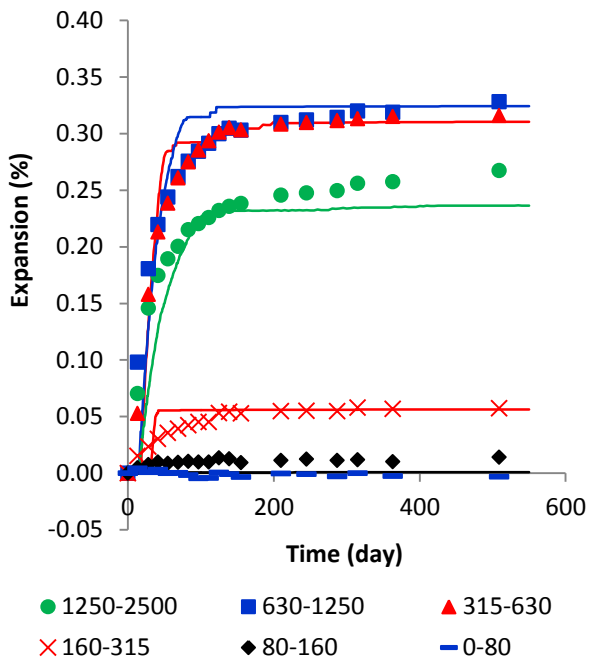

Figure **13**: Expansion according to aggregate size [59] (points) and numerical modelling (curves)

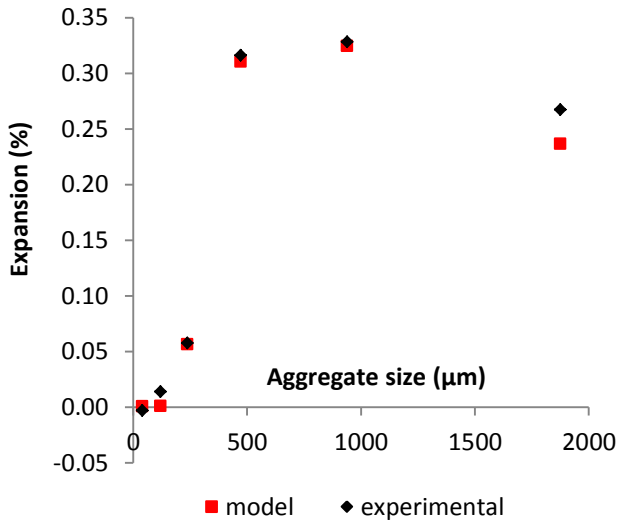

Figure **14**: Pessimum effect in expansion due to aggregate size, experimentation and modelling